ISSN 1063-7788, Physics of Atomic Nuclei, 2015, Vol. 78, No. 8, pp. 905–911. © Pleiades Publishing, Ltd., 2015.
Original Russian Text © D.A. Kasatov, A.N. Makarov, S.Yu. Taskaev, I.M. Shchudlo, 2015, published in Yadernaya Fizika, 2015, Vol. 78, No. 11, pp. 963–969.

NUCLEI
Experiment

Radiation Accompanying the Absorption of 2-MeV Protons in Various Materials

D. A. Kasatov[1),2)], A. N. Makarov[1)], S. Yu. Taskaev[1),2)*], and I. M. Shchudlo[1)]

Received March 6, 2015

Abstract—For the development of boron neutron-capture therapy of malignant tumors, a source of epithermal neutrons on the basis of a tandem accelerator with a vacuum insulation and a lithium target was created and launched. With the aim of optimizing the neutron-producing target, various structure materials were irradiated with a proton beam. The results obtained by measuring the dose rate and radiation spectrum upon the absorption of 2-MeV protons are presented, and the choice of tantalum for an optimum material of the target substrate was explained.

DOI: 10.1134/S1063778815080062

1. INTRODUCTION

Boron neutron-capture therapy is a promising procedure for the treatment of malignant tumors [1]. This method ensures a selective destruction of tumor cells via a preliminary accumulation in them of the stable nonradioactive isotope ^{10}B and subsequent irradiation with neutrons. Neutron absorption by boron gives rise to a nuclear reaction accompanied by a high energy deposition in tumor cells. Intense fluxes of epithermal neutrons are required for the treatment of deeply seated tumors. The threshold reaction $^{7}\mathrm{Li}(p,n)^{7}\mathrm{Be}$ induced by 2- to 2.5-MeV protons provides the best means for the production of such neutrons. In addition to neutron production, proton interaction with lithium nuclei leads to a sizable emission of 0.478-MeV photons [2]. In order to reduce this undesirable accompanying flux of photons, the thickness of the neutron-producing lithium layers should be such that protons in it were moderated to the neutron-production threshold of 1.882 MeV. Further, it is required that the protons be thereupon absorbed in materials where photons are not sizably produced in (p,γ), $(p,p'\gamma)$, $(p,n\gamma)$, and $(p,\alpha\gamma)$ reactions [3]. The objective of the present study was to explore experimentally radiation accompanying the absorption of 2-MeV protons in various materials in order to choose such a structural material for the substrate of the neutron-producing target that would ensure a minimum yield of accompanying gamma radiation.

2. EXPERIMENTAL RESULTS AND DISCUSSIONS

The investigations reported here were performed at a tandem accelerator with vacuum insulation which was proposed and constructed for the development of boron neutron-capture therapy [4]. At the accelerator, a proton beam 1 cm in diameter and of energy and current 2 MeV and up to 1.6 mA, respectively, is obtained in a stable long-term regime [5]. The beam is

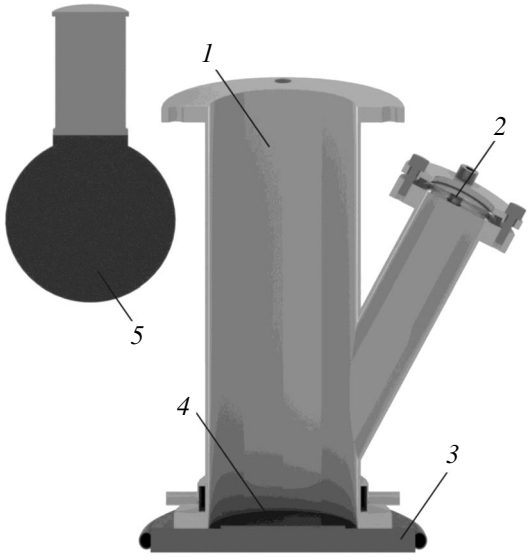

Fig. 1. Layout of the experimental setup used: (*1*) vacuum volume, (*2*) window for observation, (*3*) cooled bottom of the vacuum volume, (*4*) sample, and (*5*) spherical ionization chamber.

[1)]Budker Institute of Nuclear Physics, Siberian Branch, Russian Academy of Sciences, pr. Akademika Lavrentieva 11, Novosibirsk, 630090 Russia.
[2)]Novosibirsk State University, ul. Pirogova 2, Novosibirsk, 630090 Russia.
*E-mail: taskaev@inp.nsk.su

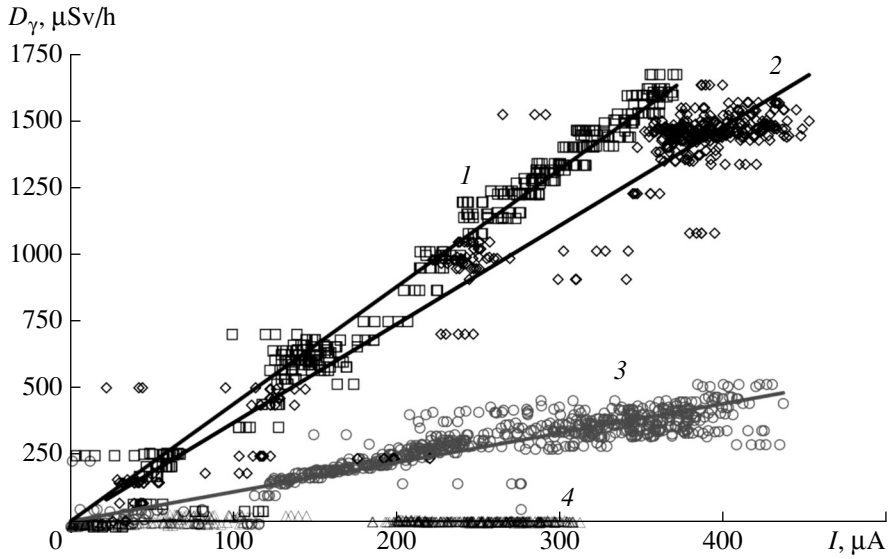

Fig. 2. X-ray and gamma-radiation dose rate versus the proton-beam current upon the irradiation of (*1*, open boxes) vanadium, (*2*, open diamonds) titanium, (*3*, open circles) stainless steel, and (*4*, open triangles) tantalum.

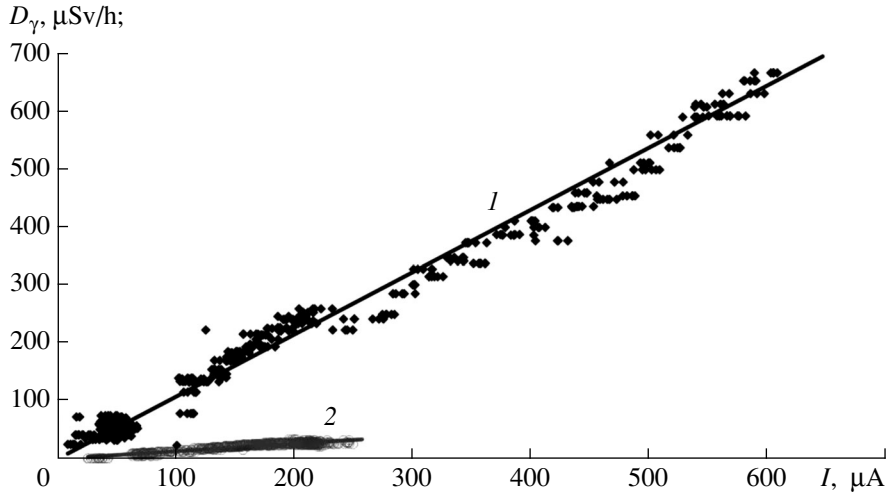

Fig. 3. Radiation-dose rate as a function of the proton-beam current upon the irradiation of a neutron-generating target for the cases where (*1*) lithium is sputtered onto the copper target substrate and (*2*) use is made of a pure-copper substrate.

highly monochromatic in energy 0.1%, and its current is highly stable (0.5%). In order to perform the investigations in question, a neutron-producing target [6] was replaced by a specially designed vacuum volume (see Fig. 1) consisting of a stainless-steel pipe and a sleeve with a quartz glass for observation. The pipe had an inner diameter of 100 mm and a wall thickness of 2 mm. Its bottom from a copper disk 16 mm thick was cooled with water.

Various materials manufactured predominantly in the form of thin disks 95 mm in diameter were placed on the bottom of the vacuum volume and, by means of magnetic scanning, were irradiated with a 2 MeV proton beam of current up to 500 μA. A web camera permitted observing the sample-surface state and, in a number of cases, beam scanning uniformity by the glow of the sample. The absorbed dose of electromagnetic radiation was measured at a distance of 25 cm from the sample center by a spherical ionization chamber that is similar to that which was described in [7], while the neutron-radiation dose was measured at a distance 50 cm by a DKS-96 radiometric dosimeter equipped with a BDMN-96 detection block. Since the readings of the ionization chamber received a contribution from the radiation of the accelerator used, there was a need for determining this contribution. This was done with the aid of a different ionization chamber that was positioned re-

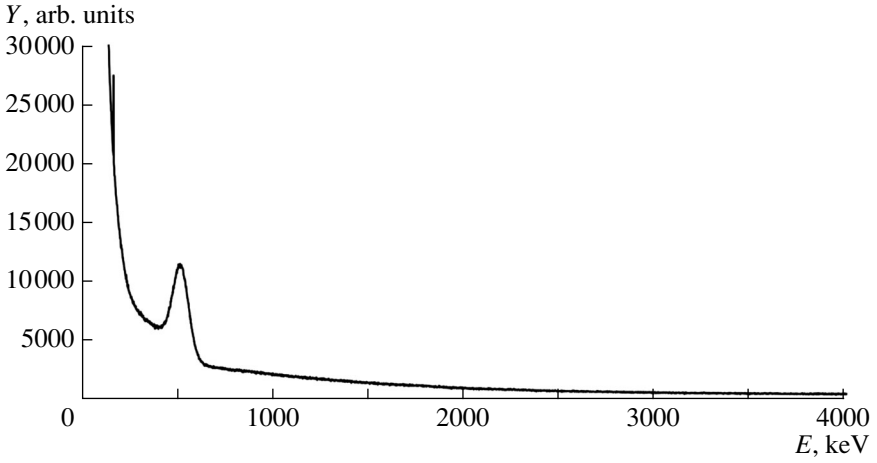

Fig. 4. Spectrum of gamma radiation from barium fluoride irradiated with a beam of 2-MeV protons.

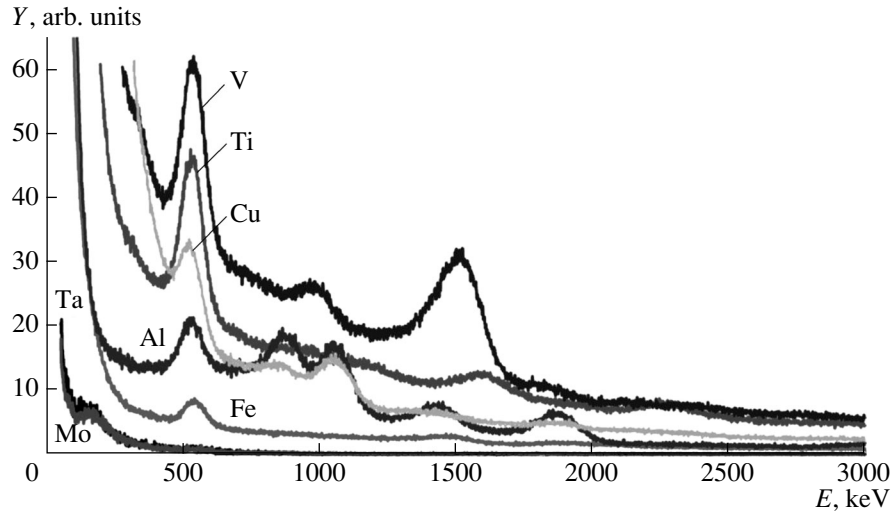

Fig. 5. Spectrum of gamma radiation from the following materials irradiated with a beam of 2-MeV protons: vanadium (V), titanum (Ti), copper (Cu), aluminum (Al), stainless steel (Fe), tantalum (Ta), and molibdenum (Mo).

motely from the irradiated samples and in which only bremsstrahlung from the accelerator was recorded [8]. Figure 2 shows the x-ray and gamma-radiation dose rates (upon the subtraction of the contribution of the accelerator contribution) as a function of the proton-beam current for various samples. One can see that the dose rate grows linearly with the beam current.

Constructing least squares fit to data (see straight lines in Fig. 2), we determine the dose rates per current unit for all materials being studied. They are given in the table. The table also presents the errors in determining the dose rate that characterize the spread of experimental data. It should be noted that data for lithium were obtained by using a neutron-producing target [6]. The dose rate was first measured without an evaporated lithium layer, in which case protons were absorbed in the copper substrate of the target; thereupon, it was measured with an evaporated layer 50 μm thick from pure metallic lithium (see Fig. 3) [9, 10]. From the table, it can be seen that the absorption of 2-MeV protons in structural materials is accompanied by a substantially lower dose rate in relation to the case of lithium.

A sizable rate of radiation from barium fluoride and lithium fluoride crystals is worthy of special note. In order to rule out errors, the radiation dose was measured anew with an LB6500-3H-10 (Berthold Tech.) gamma detector. These crystals were not considered as candidates for target structural materials, but they were subjected to irradiation with a proton beam in order to test experimentally the possibility of the generation of a strong positron beam [11]. It is commonly known that proton interaction with fluorine leads to the production of a ^{20}Ne nucleus, which decays to an

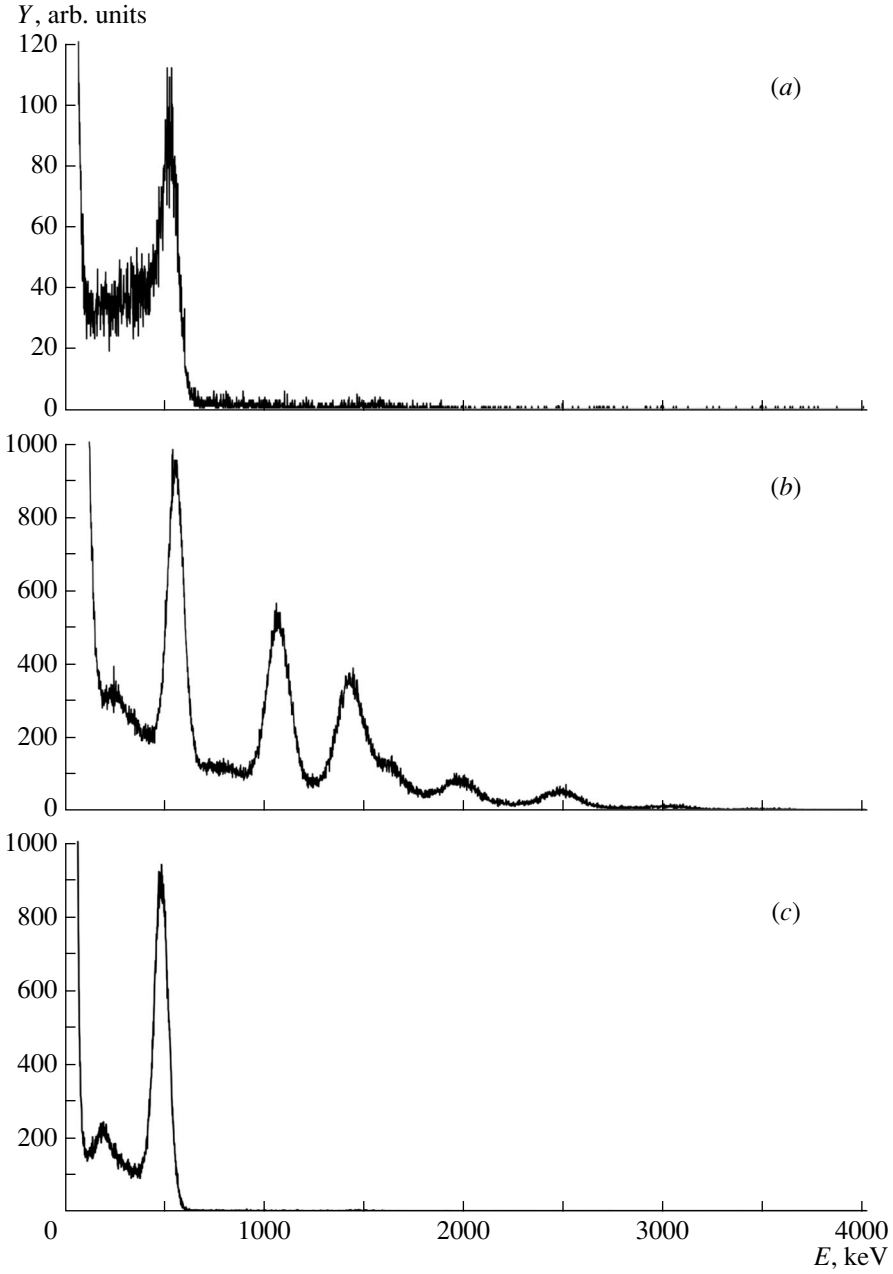

Fig. 6. Residual-activity spectrum of gamma radiation from (*a*) graphite, (*b*) titanum, and (*c*) lithium fluoride.

alpha particle and a ^{16}O nucleus in the excited state at the excitation energy of 6.05 MeV. This excitation is removed via the emission of an electron–positron pair. We can represent this reaction in the form $^{19}\mathrm{F}(p,\alpha e^{+}e^{-})^{16}\mathrm{O}$; its cross section reaches 0.2 b at the proton energy of 2 MeV. Spectra of gamma radiation caused by the absorption of 2-MeV protons in barium fluoride are shown in Fig. 4 according to measurements with a BGO spectrometer (scintillator 80 mm in diameter and 100 mm in height) positioned under the vacuum volume; 511-keV photons originating from the annihilation of product positrons can clearly be seen in this scintillator. This property of the generation of a strong photon flux can be used for the diagnostics of the current or the current profile of a proton beam—for example, by measuring the gamma-radiation dose rate upon the introduction of a fluorine-containing sample in the beam.

Spectra of gamma radiation induced by the absorption of 2-MeV protons in structural materials are shown in Fig. 5 according to measurements with a BGO gamma spectrometer. We recall that proton absorption in lithium leads to the formation of a monochromatic flux of 478-keV photons. The re-

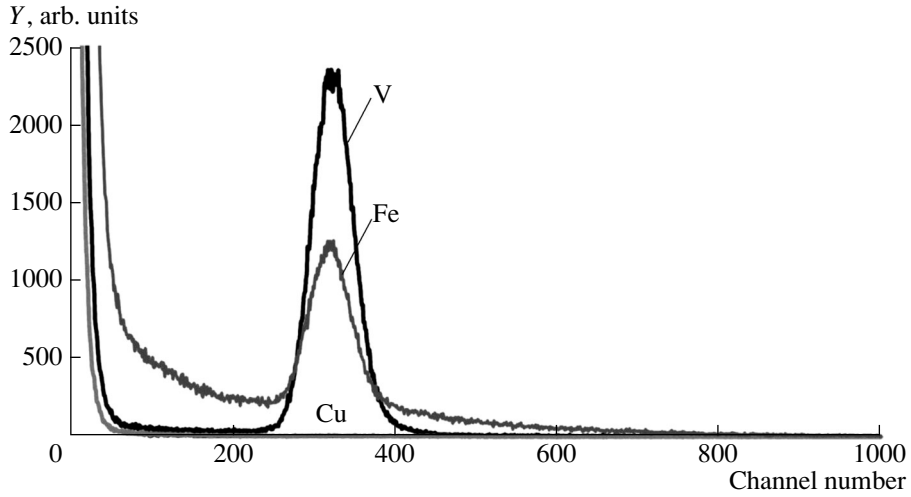

Fig. 7. Counting rate in a neutron detector as a function of the channel number (energy) upon the irradiation of copper (Cu), stainless steel (Fe), and vanadium (V) with 2-MeV protons.

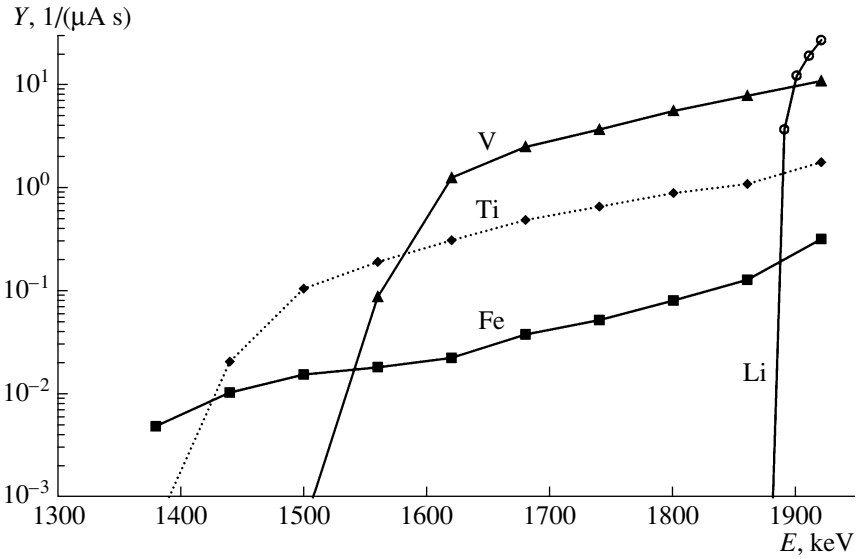

Fig. 8. Detector counting rate in the neutron-peak region as a function of the energy of protons absorbed in vanadium (V), titanium (Ti), stainless steel (Fe), and lithium (Li).

spective experimental results were presented in [12]. Figure 5 shows that there is virtually no radiation from molybdenum and tantalum.

Figure 6 gives the residual-activity spectra for graphite, titanium, and lithium fluoride. No sizable activity was observed in other materials. It turned out that the activation of graphite, titanium, and lithium fluoride was due to, respectively, the process $^{12}\mathrm{C}(p)\,^{13}\mathrm{N} \xrightarrow{\beta^+(10\ \mathrm{min})} {}^{13}\mathrm{C}$; proton absorption by the isotopes ^{46}Ti and ^{47}Ti, which is followed by the β^+ decay of ^{47}V and ^{48}V nuclei and electron capture in ^{48}V [13]; and the production of the radioactive isotope ^{7}Be in the reaction $^{7}\mathrm{Li}(p,n)^{7}\mathrm{Be}$. Titanium activation by a proton beam can also be used for diagnostic purposes in order to measure the charge transferred by the beam.

The irradiation of stainless steel, titanium, and vanadium with 2-MeV protons was found to lead to neutron production, but the irradiation of other materials was not accompanied by the yield of neutrons. The absorbed dose rate was measured with a DKS-96 radiometric dosimeter. For vanadium, the result was 7000 μSv/(h m^2 mA), while, for stainless steel, it was smaller by a factor of 25. Neutron production was confirmed by the presence of a characteristic signal from the reaction $^{6}\mathrm{Li} + n \rightarrow$

Rate of gamma-radiation dose absorbed by various materials exposed to 2-MeV protons

Material (mass number)	Dose rate per current unit, D_γ, μSv/(h m^2 mA)	Errors in determining dose rates, %
Lithium fluoride	20 000	20
Barium fluoride	6500	20
Lithium layer 50 μm thick on copper substrate	750	5
Graphiteит	25	10
Aluminum (27)	150	5
Silicon (28)	23	2
Titanium (48)	230	8
Vanadium (51)	270	4
Stainless steel 12X18H10T	70	10
Copper (64)	90	5
Molybdenum (96)	<6	
Tantalum (181)	<6	

$^3\mathrm{H} + \alpha + 4.785$ MeV in a detector (channel nos. 300–400 in Fig. 7) based on a GS20 scintillator 18 mm in diameter and 4 mm in thickness (The Saint-Gobain Crystals, USA). Figure 8 shows the detector counting rate in the region around this neutron peak as a function of the proton energy. From the resulting dependences, it follows that neutron production in stainless steel was due to the reaction $^{55}\mathrm{Mn}(p,n)^{55}\mathrm{Fe}$ (the reaction threshold is 1.034 MeV); in titanium and vanadium, this was due to, respectively, the reaction $^{49}\mathrm{Ti}(p,n)^{49}\mathrm{V}$ (the reaction threshold is 1.43 MeV) and the reaction $^{51}\mathrm{V}(p,n)^{51}\mathrm{Cr}$ (the reaction threshold is 1.562 MeV). Since the thresholds for these reactions is substantially lower than the threshold for the reaction $^7\mathrm{Li}(p,n)^7\mathrm{Be}$, the energies of neutrons originating from them are higher than the energies of neutrons emitted by lithium. For this reason, it is not wise to use stainless steel, titanium, or vanadium as materials for the substrate of the neutron-producing target. The point is that the system intended for forming an epithermal-neutron beam [14] was tuned to moderating neutrons from the reaction $^7\mathrm{Li}(p,n)^7\mathrm{Be}$, so that fast neutrons will not be moderated properly by this system. As a result, an additional undesirable dose from fast neutrons would appear in performing therapy.

Thus, the application of tantalum or molybdenum as materials for the substrate of the neutron-producing target would ensure a minimum level of undesirable gamma radiation, the absence of an undesirable fast-neutron flux, and the absence of material activation. In choosing a target material, it is also necessary to take into account its strength against radiation damage (blistering) in the implantation of protons. Since the deceleration of protons in metals proceeds nearly along a straight line, all of them undergo stopping at the same depth. Therefore, the captured gas atoms are agglomerated, and the surface layer may be deformed up to the formation of blisters (small domelike structures on the surface) and the exfoliation of the surface because of an increase in the internal pressure and a side compression stress. As a rule, blistering is observed in metals that dissolve hydrogen purely—in particular, in molybdenum [15]. As was shown in [16], tantalum, along with vanadium and alpha iron, has the highest strength against blistering upon the absorption of 2-MeV protons in the case where the temperature of the metals is about 150°C, which is characteristic of a target heated by a proton beam and cooled by a turbulent flow of water [6]. In view of these two circumstances, the application of tantalum as a material for manufacturing, for a neutron-producing target, a substrate onto which a thin lithium layer is evaporated and in which protons are absorbed is the best solution in an accelerator source of epithermal neutrons for boron neutron-capture therapy.

3. CONCLUSIONS

Samples manufactured from lithium, graphite, magnesium fluoride, barium fluoride, aluminum, silicon, titanium, vanadium, stainless steel, copper,

molybdenum, and tantalum have been exposed to a proton beam at a tandem accelerator with vacuum insulation. The x-ray and gamma-radiation dose rates and spectra and the neutron-emission dose rate upon the absorption of 2-MeV protons in various materials have been measured along with the residual-activity radiation spectrum. The emission of neutrons from lithium, vanadium, stainless steel, and titanium and the activation of lithium, graphite, and titanium have been detected. We have found that the absorption of 2-MeV protons in molybdenum or tantalum proceeds at a minimum dose-rate level of accompanying x-ray and gamma radiation and does not lead to the production of fast neutrons and to a residual activity. With allowance for earlier investigations into the blistering phenomenon, we recommend tantalum as a material for the substrate of a lithium neutron-producing target for boron neutron-capture therapy since tantalum gives a minimum flux of undesirable radiation and possesses the highest strength against radiation damage.

ACKNOWLEDGMENTS

This work was funded by the Russian Science Foundation (project no. 14-32-00006) under support of the Budker Institute of Nuclear Physics (Siberian Branch, Russian Academy of Sciences).

REFERENCES

1. *Neutron Capture Therapy. Principles and Applications*, Ed. by W. Sauerwein, A. Wittig, R. Moss, and Y. Nakagawa (Springer, Heidelberg, New York, Dordrecht, London, 2012).
2. V. N. Kononov, M. V. Bokhovko, O. E. Kononov, et al., Preprint FEI-2643 (Inst. Phys. Power Eng., Obninsk, 1997).
3. A. Savidou, X. Aslanoglou, T. Paradellis, and M. Pilakouta, Nucl. Instrum. Methods Phys. Res. B **152**, 12 (1999).
4. B. F. Bayanov, V. P. Belov, E. D. Bender, et al., Nucl. Instrum. Methods Phys. Res. A **413**, 397 (1998).
5. D. Kasatov, A. Kuznetsov, A. Makarov, I. Shchudlo, I. Sorokin, and S. Taskaev, J. Instrum. **9**, P12016 (2014).
6. B. Bayanov, V. Belov, and S. Taskaev, J. Phys.: Conf. Ser. **41**, 460 (2006).
7. V. G. Barkova, O. M. Koryabkin, A. V. Repkov, and V. Ya. Chudaev, in *Proceedings of the 9th All-Union Workshop on Accelerators of Charged Particles* (Dubna, 1985), Vol. 2, p. 318.
8. D. A. Kasatov, A. N. Makarov, S. Yu. Taskaev, and I. M. Shchudlo, Tech. Phys. Lett. **41**, 139 (2015).
9. B. F. Bayanov, E. V. Zhurov, and S. Yu. Taskaev, Instrum. Exp. Tech. **51**, 147 (2008).
10. B. F. Bayanov, S. Yu. Taskaev, V. I. Obodnikov, and E. G. Tishkovskii, Instrum. Exp. Tech. **51**, 438 (2008).
11. P. Farrell, V. Dudnikov, N. Guardala, et al., in *Proceedings of the 7th International Workshop on Positron and Positronium Chemistry (PPC-7), Knoxville, USA, 2002* (Pergamon, 2003), p. 47.
12. A. S. Kuznetsov, G. N. Malyshkin, A. N. Makarov, I. N. Sorokin, Yu. S. Sulyaev, and S. Yu. Taskaev, Tech. Phys. Lett. **35**, 346 (2009).
13. *Tables of Physical Quantities, Reference Book,* Ed. by I. K. Kikoin (Atomizdat, Moscow, 1976) [in Russian].
14. V. Aleynik, A. Bashkirtsev, V. Kanygin, D. Kasatov, A. Kuznetsov, A. Makarov, I. Schudlo, I. Sorokin, S. Taskaev, and M. Tiunov, Appl. Radiat. Isot. **88**, 177 (2014).
15. M. I. Guseva and Yu. V. Martynenko, Sov. Phys. Usp. **24**, 996 (1981).
16. V. T. Astrelin, A. V. Burdakov, P. V. Bykov, et al., J. Nucl. Mater. **396**, 43 (2010).